13th World Conference on Earthquake Engineering
Vancouver, B.C., Canada
August 1-6, 2004
Paper No. 202

NEW MODEL FOR THE INELASTIC BIAXIAL BENDING OF REINFORCED CONCRETE COLUMNS

Xavier ROMÃO[1], Aníbal COSTA[2], Raimundo DELGADO[3]

SUMMARY

A model is proposed for the force-deformation behaviour of reinforced concrete members under biaxial loading with axial force. It embodies an existing uniaxial hysteretic model with piecewise linear behaviour as the foundation for its development and proceeds from analogy and comparison with the biaxial formulation of the Bouc-Wen smooth hysteretic model previously presented by other authors.
The proposed biaxial model formulation requires the same information needed for the corresponding uniaxial model and introduces an additional correcting term into the existing uniaxial model coupling the two loading directions. The validity of the presented model is demonstrated through the analytical simulation of available biaxial experiments on reinforced concrete columns. The presented model is proven to be efficient and establishes a simple form of analysing reinforced concrete structures in which biaxial interaction should be considered.

INTRODUCTION

There are still a number of unsolved problems standing in the way of the adequate modeling of reinforced concrete (RC) buildings under general earthquake loading. One of the main issues is related to the fact that buildings are tridimensional structures and in several cases the simplification of the tridimensional models into bidimensional ones without much loss of accuracy is impossible. In many situations biaxial structural interaction and torsional oscillation may arise, namely as a result of structural irregularity, affecting the structural response. However, even for structures with regular and symmetric configurations and uniform mass distributions in the building plan, planar models cannot be considered in order to obtain a response accurate enough. Since earthquake excitation is, in general, multi-dimensional, biaxial structural interaction must, therefore, be considered.
The behavior of structural elements, especially axially loaded RC members, under biaxial loading histories is important, not only because the real response of specific members is in many cases tridimensional, but because the biaxiality of the loading leads to a reduction of the bearing capacity of the member, while increasing the stiffness and strength degradation usually present with cycling. The inelastic behavior of

[1] Research Assistant, Faculdade de Engenharia da Universidade do Porto, Portugal. Email: xnr@fe.up.pt.
[2] Aggregate Professor, Faculdade de Engenharia da Universidade do Porto, Portugal. Email: agc@fe.up.pt.
[3] Full Professor, Faculdade de Engenharia da Universidade do Porto, Portugal. Email: rdelgado@fe.up.pt.

vertical members, in particular of columns, is, therefore, of special interest and requires nonlinear member models able to represent their behavior under generalized cyclic biaxial bending with axial loading.
Nonlinear dynamic analysis in three dimensions is still very limited, not only due to the higher requirements in computer time, but also because there is a lack of relatively simple models that can accurately and reliably define the complex behavior of vertical members under inelastic biaxial bending with axial force. Adding one more dimension to the problem of uniaxial flexure considerably increases its complexity and the difficulty of developing simple analytical models. As a consequence, it has been seen over the years that the development of phenomenological rules in three dimensions able to reproduce experimentally observed behavior, like the ones available for the bidimensional problems, has been short on success.
Fibre models constitute the major category of models used in tridimensional analyses. These models can capture the full coupling of the two bending directions with the axial force. However, their requirements in computer time and input preparation are much higher than those of macroelements based on empirical moment-curvature or force-deformation relations. Moreover, only recent more advanced fibre models [1] take into account the effects of the shear deformations and bond slip. Therefore, despite the great power of fibre models, there is still room for development and application of simpler models for RC members, since the simulation of the global seismic response must essentially reproduce the member effective stiffness and energy dissipation as a function of the deformation level.
Excluding fibre models, the present state-of-the-art in modeling RC members under cyclic biaxial bending with axial load is far behind that of the uniaxial flexure. A detailed review of experimental results and models for cyclic biaxial bending of RC members with axial force is presented in [2].
Outside the theory of fibre models, the existent analytical models follow the concepts of Classical Plasticity [3], Mroz's Multisurface Plasticity [4, 5, 6], Bouc-Wen's [7] hysteresis model [8, 9, 10], Bounding Surface Plasticity [11, 12, 13] or lumped damage mechanics [14].
Since engineers performing nonlinear dynamic planar analyses with piecewise linear (PWL) models are more familiar with these type of models, it seems important, for the purpose of upgrading to tridimensional analyses, to try to develop a framework of biaxial models where PWL models can fit. The present paper proposes a new model for biaxial bending with axial force that is an extension of an existing uniaxial hysteretic model with PWL behavior. The general formulation of the model proceeds from analogy and comparison with the biaxial formulation of the Bouc-Wen smooth hysteretic model [9]. Although retaining most of the physical meaning embodied in the Bouc-Wen model, the presented framework adds simplicity and versatility since many of the existing PWL models can be used with this formulation.
The model formulation is presented in a general force-displacement form to be in agreement with the experimental results selected to test the performance of the model. However, the specific biaxial bending form is easily obtained by expressing the force and displacement as moment and curvature.

THE BIAXIAL BOUC-WEN MODEL AS A BASIS FOR THE PROPOSED MODEL

The basic format of the Bouc-Wen model for uniaxial behavior was first presented by Bouc [15], later generalized by Wen [7], and involves the solution of a differential equation. The generalized model expresses the restoring force as the combination of an elastic force and a plastic force

$$F = \alpha \cdot K \cdot u + (1 - \alpha) \cdot F^{y} \cdot Z \tag{1}$$

where K is the initial stiffness, α is the post-yield stiffness ratio, F_y is the yield force, and Z is the hysteretic parameter given by

$$\dot{Z} = \frac{A \cdot \dot{u} - \beta \cdot |\dot{u} \cdot Z| \cdot Z^{n-1} - \gamma \cdot \dot{u} \cdot Z^{n}}{u^{y}} \tag{2}$$

in which A, γ, β and n are dimensionless parameters controlling the shape and magnitude of the hysteresis loops and u^y is the yield displacement of the system.
By rewriting Eq. (1) in its incremental form instead,

$$\dot{F} = \alpha \cdot K \cdot \dot{u} + (1-\alpha) \cdot F^{y} \cdot \dot{Z} \tag{3}$$

it can now be joined with Eq. (2) into a single expression which defines the incremental restoring force $\dot{F}_i$ for a specific displacement increment $\dot{u}_i$.

$$\dot{F}_i = \alpha \cdot K \cdot \dot{u}_i + (1-\alpha) \cdot K \cdot \left(A \cdot \dot{u}_i - \beta \cdot |\dot{u}_i \cdot Z_i| \cdot Z_i^{n-1} - \gamma \cdot \dot{u}_i \cdot Z_i^{n}\right) \tag{4}$$

The variable Z_i can be eliminated from Eq. (4) by rewriting Eq. (1) in the form

$$Z_i = \frac{F_i - \alpha \cdot K \cdot u_i}{(1-\alpha) \cdot F^{y}} \tag{5}$$

and considering that the global restoring force F_i results from:

$$F_i = F_{i-1} + \dot{F}_i \tag{6}$$

where F_{i-1} represents the global restoring force for the previous displacement increment.

Later, this uniaxial formulation was extended by Park, Wen and Ang [16] to define a biaxial force-deformation model with coupled differential equations. This model was then used and modified by Kunnath and Reinhorn [8] to model the behavior of RC columns under biaxial loads. Later on, the model was generalized by Casciati [9] and also by Wang and Wen [10] from which resulted two different formulations of the initial biaxial model. However, both forms give similar results. Since the Wang and Wen [10] formulation is simpler, it was selected to formulate the biaxial model proposed in the following. Nevertheless, the same mathematical reasoning can be applied to the Casciati [9] form.

The biaxial construction of the Bouc-Wen model by the Wang and Wen [10] form follows the same general idea as for the uniaxial case. The restoring forces for both directions are defined by

$$\begin{cases} F_x = \alpha_x \cdot K_x \cdot u_x + (1-\alpha_x) \cdot F_x^{y} \cdot Z_x \\ F_y = \alpha_y \cdot K_y \cdot u_y + (1-\alpha_y) \cdot F_y^{y} \cdot Z_y \end{cases} \tag{7}$$

in which the parameters involved have the same meaning as for the uniaxial case, Eq. (1), but are now referred to the orthogonal directions X and Y. The hysteretic parameters Z_x and Z_y are then defined by the following coupled differential equations:

$$\begin{cases} \dot{Z}_x = \dfrac{A \cdot \dot{u}_x - |\dot{u}_x| \cdot Z_x \cdot |Z_x|^{n-1} \cdot [\beta + \gamma \cdot sign(\dot{u}_x \cdot Z_x)] - |\dot{u}_y| \cdot Z_x \cdot |Z_y|^{n-1} \cdot [\beta + \gamma \cdot sign(\dot{u}_y \cdot Z_y)]}{u_x^y} \\ \dot{Z}_y = \dfrac{A \cdot \dot{u}_y - |\dot{u}_y| \cdot Z_y \cdot |Z_y|^{n-1} \cdot [\beta + \gamma \cdot sign(\dot{u}_y \cdot Z_y)] - |\dot{u}_x| \cdot Z_y \cdot |Z_x|^{n-1} \cdot [\beta + \gamma \cdot sign(\dot{u}_x \cdot Z_x)]}{u_y^y} \end{cases} \tag{8}$$

where the parameters involved have also the same meaning as for the uniaxial case and *sign()* refers to the mathematical signum function.
As for the case of the uniaxial model, Eq. (7) can also be reformulated into an incremental form:

$$\begin{cases} \dot{F}_x = \alpha_x \cdot K_x \cdot \dot{u}_x + (1 - \alpha_x) \cdot F_x^y \cdot \dot{Z}_x \\ \dot{F}_y = \alpha_y \cdot K_y \cdot \dot{u}_y + (1 - \alpha_y) \cdot F_y^y \cdot \dot{Z}_y \end{cases} \tag{9}$$

and joined with Eq. (9) to define the following system of coupled equations which express the incremental restoring orthogonal forces $\dot{F}_x$ and $\dot{F}_y$:

$$\begin{cases} \dot{F}_{x_i} = \alpha_x \cdot K_x \cdot \dot{u}_{x_i} + (1 - \alpha_x) \cdot K_x \cdot \Big[A \cdot \dot{u}_{x_i} - |\dot{u}_{x_i}| \cdot Z_{x_i} \cdot |Z_{x_i}|^{n-1} \cdot [\beta + \gamma \cdot sign(\dot{u}_{x_i} \cdot Z_{x_i})] - \\ \qquad |\dot{u}_{y_i}| \cdot Z_{x_i} \cdot |Z_{y_i}|^{n-1} \cdot [\beta + \gamma \cdot sign(\dot{u}_{y_i} \cdot Z_{y_i})] \Big] \\ \dot{F}_{y_i} = \alpha_y \cdot K_y \cdot \dot{u}_{y_i} + (1 - \alpha_y) \cdot K_y \cdot \Big[A \cdot \dot{u}_{y_i} - |\dot{u}_{y_i}| \cdot Z_{y_i} \cdot |Z_{y_i}|^{n-1} \cdot [\beta + \gamma \cdot sign(\dot{u}_{y_i} \cdot Z_{y_i})] - \\ \qquad |\dot{u}_{x_i}| \cdot Z_{y_i} \cdot |Z_{x_i}|^{n-1} \cdot [\beta + \gamma \cdot sign(\dot{u}_{x_i} \cdot Z_{x_i})] \Big] \end{cases} \tag{10}$$

In the same way as for the uniaxial case, the variables Z_{x_i} and Z_{y_i} may be eliminated from Eq. (10) by rewriting Eq. (7) in the form

$$\begin{cases} Z_{x_i} = \dfrac{F_{x_i} - \alpha_x \cdot K_x \cdot u_{x_i}}{(1 - \alpha_x) \cdot F_x^y} \\ Z_{y_i} = \dfrac{F_{y_i} - \alpha_y \cdot K_y \cdot u_{y_i}}{(1 - \alpha_y) \cdot F_y^y} \end{cases} \tag{11}$$

and considering that the global restoring forces F_{x_i} and F_{y_i} result from:

$$\begin{cases} F_{x_i} = F_{x_{i-1}} + \dot{F}_{x_i} \\ F_{y_i} = F_{y_{i-1}} + \dot{F}_{y_i} \end{cases} \tag{12}$$

FRAMEWORK OF THE PROPOSED BIAXIAL MODEL

Considering the definition of the incremental orthogonal forces $\dot{F}_{x_i}$ and $\dot{F}_{y_i}$ by Eq. (10), it can be seen, by a simple mathematical transformation, that the first part of this system

$$\begin{cases} \dot{F}_{x_i} = \alpha_x \cdot K_x \cdot \dot{u}_{x_i} + (1-\alpha_x) \cdot K_x \cdot \left(A \cdot \dot{u}_{x_i} - \left|\dot{u}_{x_i}\right| \cdot Z_{x_i} \cdot \left|Z_{x_i}\right|^{n-1} \cdot \left[\beta + \gamma \cdot sign\left(\dot{u}_{x_i} \cdot Z_{x_i}\right)\right]\right) \\ \dot{F}_{y_i} = \alpha_y \cdot K_y \cdot \dot{u}_{y_i} + (1-\alpha_y) \cdot K_y \cdot \left(A \cdot \dot{u}_{y_i} - \left|\dot{u}_{y_i}\right| \cdot Z_{y_i} \cdot \left|Z_{y_i}\right|^{n-1} \cdot \left[\beta + \gamma \cdot sign\left(\dot{u}_{y_i} \cdot Z_{y_i}\right)\right]\right) \end{cases} \tag{13}$$

matches Eq. (4) applied to the *X* and *Y* directions, thus corresponding to the uniaxial incremental restoring forces calculated for each direction without biaxial interaction. To simplify the notation, these incremental forces will be called $\dot{F}_{uni-x_i}$ and $\dot{F}_{uni-y_i}$, respectively. The remaining part of the system corresponds to the correcting factors C_{fx_i} and C_{fy_i} accounting for the interaction between the two loading directions:

$$\begin{cases} C_{fx_i} = -(1-\alpha_x) \cdot K_x \cdot \left|\dot{u}_{y_i}\right| \cdot Z_{x_i} \cdot \left|Z_{y_i}\right|^{n-1} \cdot \left[\beta + \gamma \cdot sign\left(\dot{u}_{y_i} \cdot Z_{y_i}\right)\right] \\ C_{fy_i} = -(1-\alpha_y) \cdot K_y \cdot \left|\dot{u}_{x_i}\right| \cdot Z_{y_i} \cdot \left|Z_{x_i}\right|^{n-1} \cdot \left[\beta + \gamma \cdot sign\left(\dot{u}_{x_i} \cdot Z_{x_i}\right)\right] \end{cases} \tag{14}$$

Based on Eq. (13) and (14) a condensed form of Eq. (10) can, therefore, be defined as

$$\begin{cases} \dot{F}_{x_i} = \dot{F}_{uni-x_i} + C_{fxi} \\ \dot{F}_{y_i} = \dot{F}_{uni-y_i} + C_{fyi} \end{cases} \tag{15}$$

Considering that the incremental forces $\dot{F}_{uni-x_i}$ and $\dot{F}_{uni-y_i}$ can be obtained by any kind of uniaxial hysteretic model, especially PWL models which are more common, the presented framework introduces a simple and flexible form to treat biaxial bending. This formulation requires the same information needed for the corresponding uniaxial PWL model and only introduces an additional correcting term coupling the two loading directions.

Since the uniaxial hysteretic model that may be considered to obtain the incremental forces $\dot{F}_{uni-x_i}$ and $\dot{F}_{uni-y_i}$ may be very different from the initial uniaxial Bouc-Wen formulation, the amount of biaxial interaction between may also be different. To take this into account, an additional parameter δ varying between 0 and 1 was introduced in Eq. (15) to scale the amount of interaction between the two loading directions. The final formulation of the proposed method is then defined by Eq. (16). The values of the scaling factor δ will be defined when presenting the experimental and numerical results of the biaxial tests simulations.

$$\begin{cases} \dot{F}_{x_i} = \dot{F}_{uni-x_i} + \delta \cdot C_{fx_i} \\ \dot{F}_{y_i} = \dot{F}_{uni-y_i} + \delta \cdot C_{fy_i} \end{cases} \tag{16}$$

For each vector of displacement increments $(\dot{u}_{x_i};\dot{u}_{y_i})$, the incremental forces $\dot{F}_{uni-x_i}$ and $\dot{F}_{uni-y_i}$ can be separately calculated. Next, for a given value of the δ scaling factor, the correcting factors C_{fx_i} and C_{fy_i} are evaluated by solving the system of differential equations defined by Eq. (16). In the following application of this framework, and in order to cut down the number of variables, the shape factors γ, β and n, still necessary to find C_{fx_i} and C_{fy_i} were set to be the values suggested by Kunnath and Reinhorn [8], which are,

$$\beta = \gamma = 1/2 \tag{17}$$

and

$$n = 2 \tag{18}$$

The efficiency of the presented framework will be presented in the following by comparing numerical predictions with experimental test results. First, though, a brief review of the PWL uniaxial hysteretic model considered as the base of the proposed framework will be presented.

THE COSTA-COSTA UNIAXIAL HYSTERETIC MODEL

The framework presented in the previous section allows for any uniaxial hysteretic model to be used to simulate biaxial structural behavior since the interaction part of the global model is independent of the uniaxial part.

To perform a series of tests simulating experimental behavior of frame members under cyclic biaxial loading, the Costa-Costa uniaxial hysteretic model [2, 17] was selected. A brief description of this model is presented in the following.

This model represents a generalization of the original Takeda model [2] with a trilinear skeleton curve in monotonic loading, defined by the cracking point $(d_c;F_c)$ and the yield point $(d_y;F_y)$, and including pinching, stiffness degradation and strength degradation effects. Unloading-reloading loops prior to yielding in either direction are bilinear, with slopes equal to those of the pre-cracking and post-cracking branches in the virgin loading. After the initial yielding, pinching is modeled by first reducing the initial slope of the reloading branch, Fig. 1, heading to the most extreme point of any previous post-yield excursion in the direction of the reloading, through the multiplication of the stiffness K_s towards the previous extreme point by factor $(d_y/d_m)^\beta$, in which d_y represents the yield displacement, d_m is the maximum response displacement and β is a positive constant, thus giving

$$K_s = \frac{F_m}{d_m - d_0}(d_y/d_m)^\beta \tag{19}$$

where F_m is the force at the previous maximum response point and d_0 is the deformation at the load reversal point. Once the response point crosses the line connecting the origin and the maximum response point, the reloading branch, then, heads towards the maximum response point, Fig. 1.

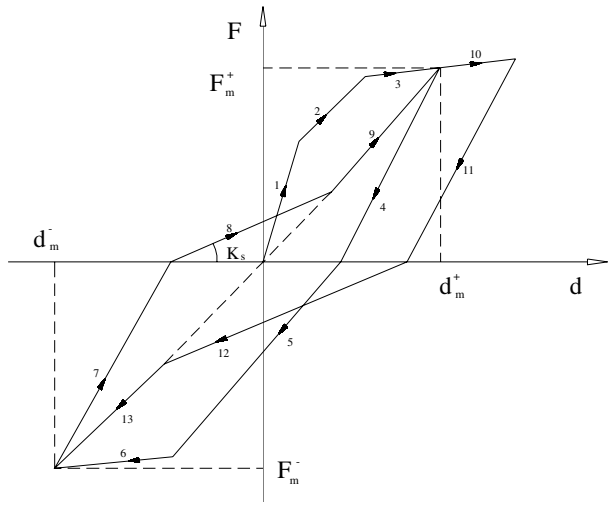

Figure 1 – Pinching effect in the Costa-Costa model.

The unloading stiffness K_d after yielding is reduced from the elastic stiffness K_e by the factor $\left(d_y/d_m\right)^{\alpha}$ where α is a positive constant, Fig. 2.

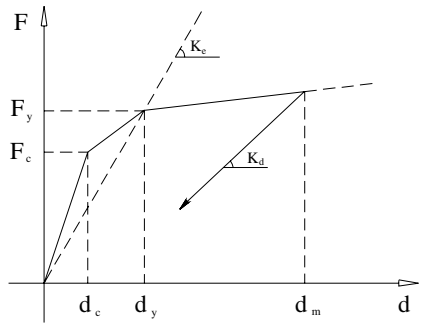

Figure 2 – Unloading stiffness degradation in the Costa-Costa model.

Post-yield strength and stiffness degradation with cycling is modeled by directing the reloading branch, after modification for pinching, towards a point at a displacement equal to d_m and at a force $F_m^{'} = \left(1-\lambda\right)\cdot F_m$, where λ is the Wang and Shah damage index [2], Fig. 3. After reaching this terminal point of the reloading branch, further loading takes place parallel to the post-yielding stiffness of the virgin loading curve.

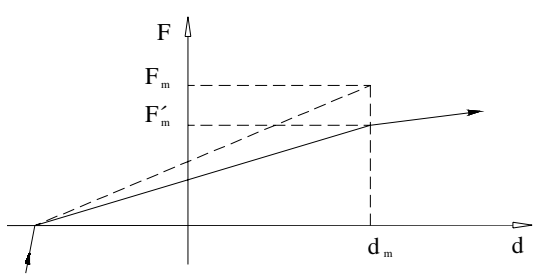

Figure 3 – Strength degradation in the Costa-Costa model.

COMPARISON OF THE BIAXIAL MODEL WITH EXPERIMENTAL TEST RESULTS

The numerical results of the proposed biaxial framework using the Costa-Costa uniaxial model were compared to experimental results performed in RC columns under complex biaxial displacement paths with constant axial force. Results from two different experimental programs were selected to carry out the evaluation.

Biaxial tests performed by Bousias *et al* [18]

Results from an intense experimental program on the behavior of RC columns under complex biaxial load paths carried out by Bousias *et al* [18] were considered to evaluate the performance of the proposed method. The specimens consisted of RC columns with a 0.25*0.25 m^2 cross section and a free length of 1.5 m and were built as cantilevers into a heavily reinforced foundation. Longitudinal reinforcement consisted of eight 16 mm diameter deformed bars uniformly distributed around the perimeter of the section. Transverse reinforcement comprised a double hoop pattern of 8 mm diameter stirrups at a 70 mm spacing. Specimens were over-designed in shear so that their behavior would be controlled by flexure. Axial loads were kept low as the values of ν, Eq. (20), where N represents the axial force, A_c is the cross section area and f_c is the uniaxial concrete compressive strength, were around 0.10. Additional details about the experimental program and results can be found in [18].

$$\nu = \frac{N}{A_c f_c} \tag{20}$$

Numerical simulation of test S1

In this test, uniaxial displacement cycles were applied alternately in the two transverse directions, in pairs of cycles with linearly increasing amplitude, Fig. 4. Figs. 5 and 6 show the hysteresis loops of both directions corresponding to the experimental results while Figs. 7 and 8 present the matching numerical predictions.

It can be observed that the experimental results of both directions are almost identical. Bousias *et al* [17] indicate that only a slight stiffness degradation in the direction of subsequent loading due to damage in the preceding cycle in the orthogonal direction was detected. This observation appears to mean that, for this test, the behavior in a specific direction is uncoupled from the behavior in the other one. This statement would also justify the reason why differences in the results were not found when using any value between 0 and 1 of the δ factor to scale the amount of interaction between the two loading directions.

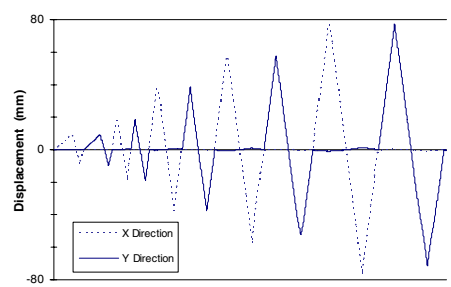

Figure 4 –Displacement cycles applied in test S1.

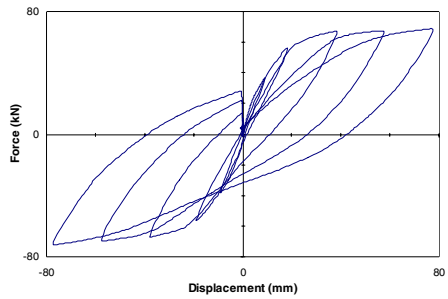

Figure 5 – Experimental hysteresis loops in X direction.

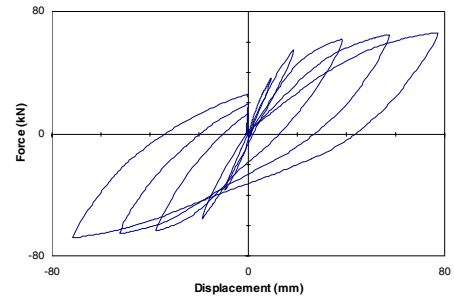

Figure 6 – Experimental hysteresis loops in Y direction.

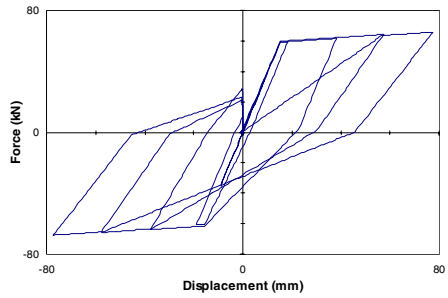

Figure 7 – Simulation of the hysteresis loops in X direction.

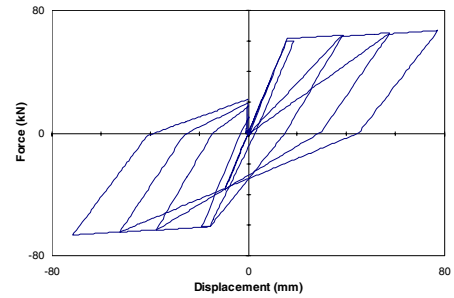

Figure 8 – Simulation of the hysteresis loops in Y direction.

Numerical simulation of test S7

In this test, the imposed biaxial deflection path is defined by concentric nested squares of increasing size, centered at the origin and traced counterclockwise. Three displacement squares were applied with half-side lengths of 40 mm, 60 mm and 80 mm, Fig. 9. Figs. 10 and 11 show the hysteresis loops of both directions corresponding to the experimental results while Fig.12 and 13 present the matching numerical predictions.

The value of the interaction scaling factor δ considered in this simulation was 0.25, which indicates a rather low coupling of the two loading directions. However, by using values of the δ factor up to 1, only the matching of the unloading and reloading stiffness is negatively affected, as strength levels remain essentially the same.

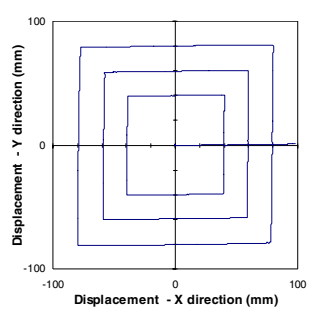

Figure 9 – Displacement cycles applied in test S7.

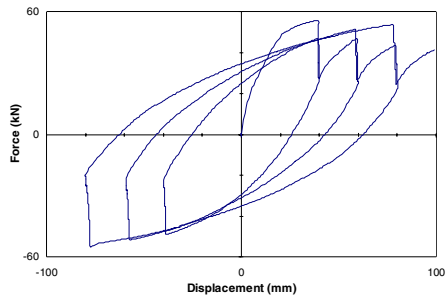

Figure 10 – Experimental hysteresis loops in X direction.

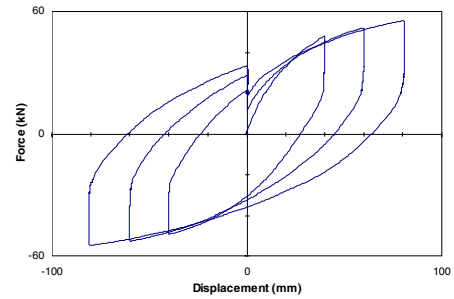

Figure 11 – Experimental hysteresis loops in Y direction.

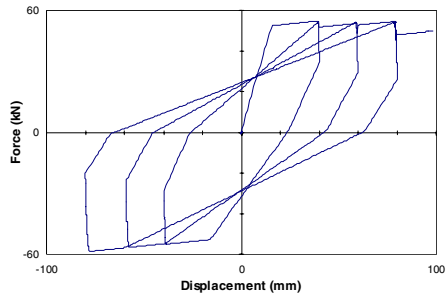

Figure 12 – Simulation of the hysteresis loops in X direction.

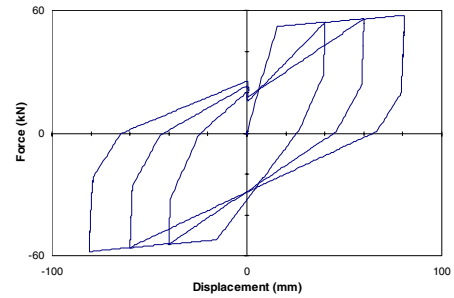

Figure 13 – Simulation of the hysteresis loops in Y direction.

Numerical simulation of test S8

As for test S8, the imposed biaxial deflection path of this test consists of concentric nested squares, centered at the origin and traced counterclockwise but now of decreasing size. Three displacement squares were applied with half-side lengths of 100 mm, 80 mm and 60 mm, Fig. 14. Figs. 15 and 16 show the hysteresis loops of both directions corresponding to the experimental results while Figs. 17 and 18 present the matching numerical predictions.

The value of the interaction scaling factor δ considered in this simulation was 0.6. However, very small variations in the overall matching of the test are obtained when increasing its value up to 1.

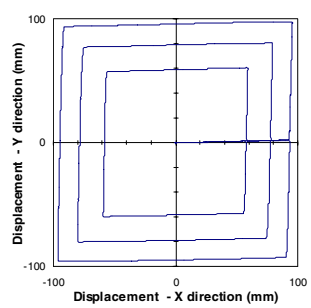

Figure 14 – Displacement cycles applied in test S8.

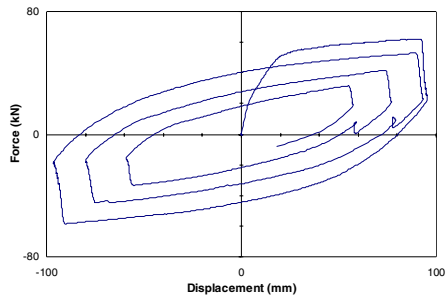

Figure 15 – Experimental hysteresis loops in X direction.

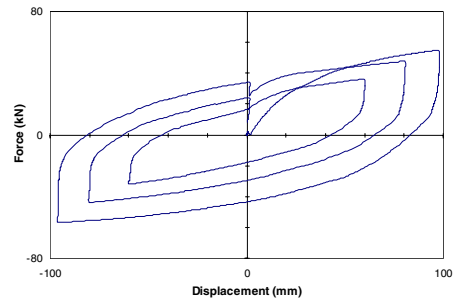

Figure 16 – Experimental hysteresis loops in Y direction.

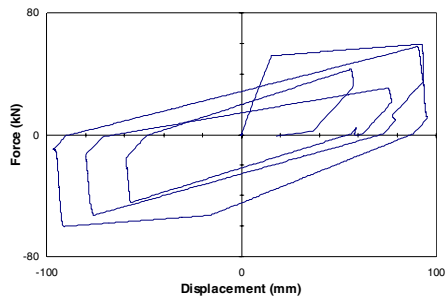

Figure 17 – Simulation of the hysteresis loops in X direction.

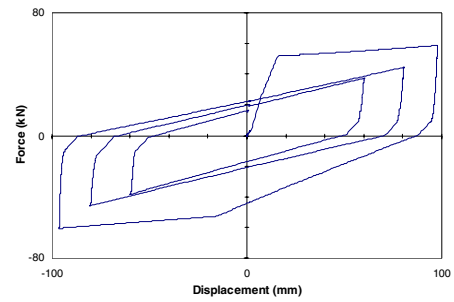

Figure 18 – Simulation of the hysteresis loops in Y direction.

Biaxial tests performed at the Kawashima Laboratory [19]

Results from an experimental program carried out at the Kawashima Laboratory of the Department of Civil Engineering at the Tokyo Institute of Technology [19] were used as a second set of results to assess the validity of the proposed biaxial model. The specimens consisted of RC columns with a 0.40*0.40 m^2 cross section and a free length of 1.75 m. Longitudinal reinforcement comprised sixteen 13 mm diameter deformed bars uniformly distributed around the perimeter of the section. Transverse reinforcement was composed by a single hoop pattern of 6 mm diameter stirrups at a 50 mm spacing. Axial loads were kept low as the values of ν were around 0.03. Additional details about the experimental program and results can be found in [19].

Numerical simulation of test TP77

The imposed biaxial deflection path for this test comprised a number of cycles defining two squares connected in the shape of an 8, Fig. 19. A set of nine 8-shaped cycles were applied and alternately traced clockwise and counterclockwise with approximate amplitudes of 3 mm, 7 mm, 13 mm, 20 mm, 25 mm, 35 mm, 40 mm, 45 mm and 55 mm, Fig. 20. Such displacement path can be seen as an alternating cross-like loading along the two diagonals, with loading and unloading along each diagonal applied in piecewise form separately along each side of the cross section. Figs. 21 and 22 show the hysteresis loops of both directions corresponding to the experimental results while Figs. 23 and 24 present the matching numerical predictions.

The value of the interaction scaling factor δ considered in this simulation was 1.0, in order to retrace as close as possible the degrading effects present with cycling that can be observed in the experimental results.

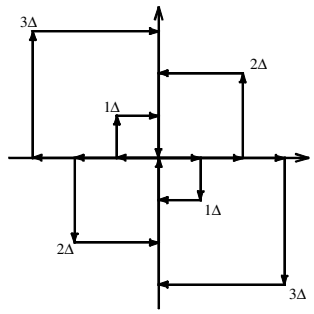

Figure 19 – Loading orbits of test TP77.

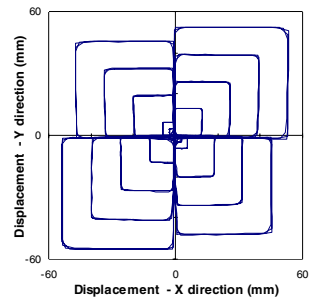

Figure 20 – Displacement cycles applied in test TP77.

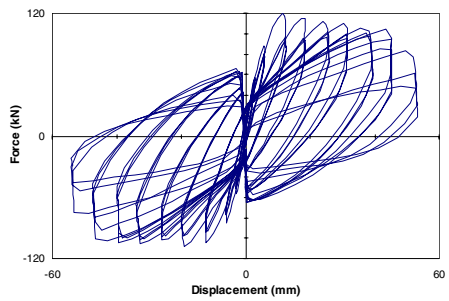

Figure 21 – Experimental hysteresis loops in X direction.

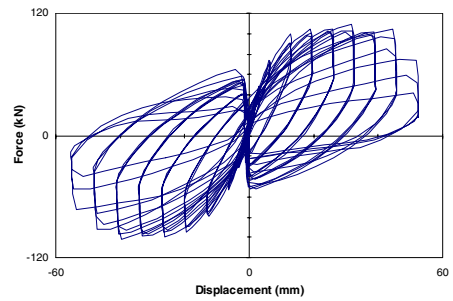

Figure 22 – Experimental hysteresis loops in Y direction.

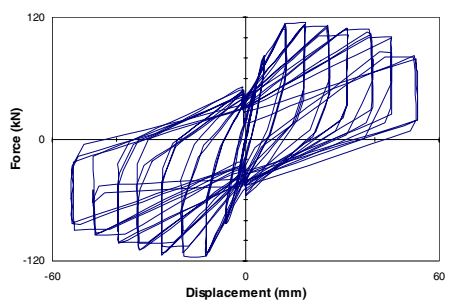

Figure 23 – Simulation of the hysteresis loops in X direction.

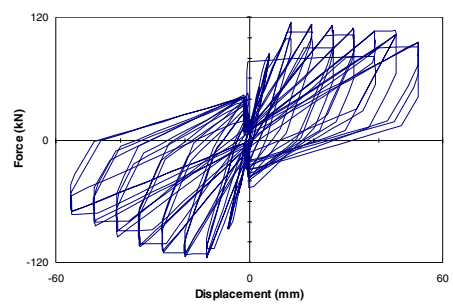

Figure 24 – Simulation of the hysteresis loops in Y direction.

Numerical simulation of test TP78

In this test, the imposed biaxial deflection path is defined by concentric nested circles of increasing size, centered at the origin and traced clockwise. Eight displacement circles were applied with radiuses around 3 mm, 6 mm, 13 mm, 20 mm, 27 mm, 34 mm, 40 mm and 47 mm, Fig. 25. Figs. 26 and 27 show the hysteresis loops of both directions corresponding to the experimental results while Figs. 28 and 29 present the matching numerical predictions.

As for the previous test, and also for the same reasons, the value of the interaction scaling factor δ considered in this simulation was 1.0.

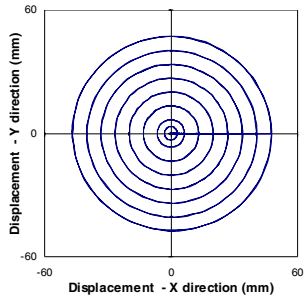

Figure 25 – Displacement cycles applied in test TP78.

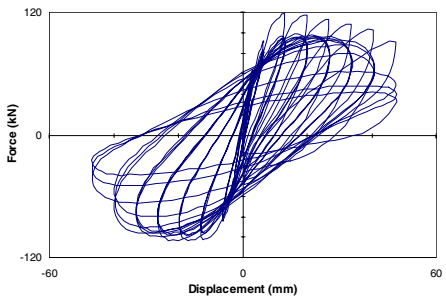

Figure 26 – Experimental hysteresis loops in X direction.

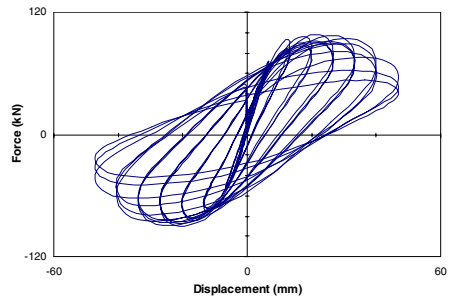

Figure 27 – Experimental hysteresis loops in Y direction.

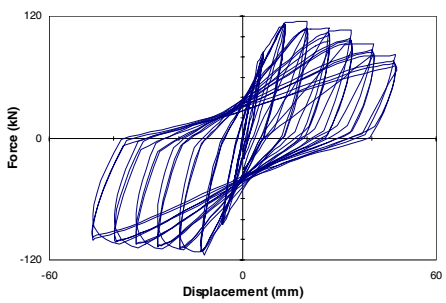

Figure 28 – Simulation of the hysteresis loops in X direction.

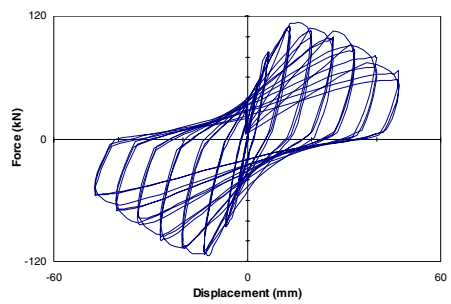

Figure 29 – Simulation of the hysteresis loops in Y direction.

DISCUSSION OF THE RESULTS

Accounting for the simplicity of the proposed biaxial model, agreement between experimental results and numerical predictions can be considered to be adequate. The overall experimentally captured coupling effects between the two loading directions as well as the general strength levels were matched by the proposed model. However, it is important to notice that the quality of the numerical results is greatly dependent of the characteristics of the uniaxial hysteretic model chosen to be the support of the proposed biaxial framework. If a model with poor correlation with uniaxial results is chosen, an adequate fitting of biaxial results cannot be expected.

Although the obtained results can be considered to be adequate, a couple of aspects still need further investigation.

First, the interaction scaling factor δ, which was set manually for the presented numerical simulations, was seen to vary from test to test. A more objective definition of this factor needs to be found in order to

demonstrate the full strength of the proposed framework and effectiveness in the analysis of the inelastic response of RC members and structures.
Second, by examining the presented experimental results, it can be seen that in almost all of the columns a decrease of the strength capacity of the virgin load curve is present when a previous loading stage occurs in the orthogonal direction. In rough terms, one can say that the yield force of the monotonic curve of a specific loading direction decreases when the member is first damaged in the orthogonal direction. This effect is not captured adequately enough by the proposed model as can be seen, for example, by comparison of Figs. 6 and 8, or 11 and 13, or 16 and 18. The modeling of the structural coupling of the two loading directions is not enough to simulate this effect since it is essentially tied to the value of the yield force assumed by the uniaxial model. As an attempt to justify this strength degradation effect, Marante and Florez-Lopez [14] stated that the axial load variation that would have probably occurred during the tests was responsible for the differences in the strength levels. Although the effect of varying axial load is an important one in the cyclic behavior of RC members, it is of the authors' knowledge that this was not the case, since the measured axial force variations during the tests were very small. To strengthen the validity and effectiveness of the proposed framework, specific degradation rules coupling the two loading directions should be defined to suitably scale the virgin load curves, this way allowing for better fitting of experimental results.

With respect to the sensitivity of the uniaxial model parameters α, β and λ, some final remarks should be presented. With respect to the α parameter, responsible for the unloading stiffness degradation, it was seen that using values similar to the ones considered in normal uniaxial behavior gives similar results. However, this was not the case for the λ parameter responsible for the strength degradation. Since most of the strength degradation occurring with cycling is captured by coupling the two loading directions, the necessary values of the λ parameter are usually smaller that the ones used in uniaxial behavior and in some cases, its consideration may even be unnecessary. Regarding the β parameter responsible for the simulation of pinching effects, since none of the experimental results exhibited specific degradation effects due to shear forces, this parameter was not considered in the simulations.

CONCLUSIONS

The present paper introduces a new approach for the behavior of biaxially loaded RC members. The proposed framework establishes an extension of existing PWL uniaxial hysteretic models and uses the biaxial structural interaction form of the Bouc-Wen biaxial hysteretic model to couple the two loading directions. The main asset of the proposed concept is the possibility to integrate any given uniaxial hysteretic model to form a global biaxial model. Since PWL uniaxial models play an important role in the nonlinear analysis of planar structures, their integration in biaxial modelling frameworks is of interest.

The Costa-Costa PWL uniaxial hysteretic model was selected to integrate the proposed biaxial framework. This model represents a generalization of the original Takeda model with a trilinear skeleton curve in monotonic loading and including pinching, stiffness degradation and strength degradation.

The validity of the presented model was demonstrated through the analytical simulation of available biaxial experiments on RC columns. The obtained numerical results were adequate and proven the model to be efficient, thus establishing a simple form of analysing RC structures in which biaxial interaction should be considered. However, additional research is still necessary to objectively define the interaction scaling factor which rules the coupling of the two loading directions and seems to exhibit a close relation with the loading history. Also, to capture with more accuracy the decrease of the strength capacity of the virgin load curve witnessed when a previous loading stage occurs in the orthogonal direction, specific

degradation rules coupling the two loading directions should be defined to suitably scale the virgin load curves, this way allowing for better fitting of experimental results.

ACKNOWLEDGMENTS

The authors would like to express their gratitude to Dr. Stathis Bousias from the University of Patras and Dr. Artur Pinto from the Joint Research Centre at Ispra for providing the set of results from the experimental program carried out at the ELSA laboratory.

REFERENCES

1. Petrangeli, M., Pinto, P. E. and Ciampi, V. "Fiber element for cyclic bending and shear of RC structures. I: Theory," J. Engrg. Mech., ASCE, 1999, 125(9): 994-1001.
2. CEB, "RC Frames under Earthquake Loading", 1996, Comité Euro-International du Béton, Bulletin nº231.
3. Pecknold, D. "Inelastic structural response to 2D ground motion," J. Engrg. Mech. Div., ASCE, 1974, 100(EM5): 949-963.
4. Takizawa, H. and Aoyama, M. "Biaxial effects in modelling earthquake response of R/C structures," Earthq. Engrg. Struct. Dyn., 1976, 4: 523-552.
5. Powell, G. H. and Chen, P. F. "3D beam-column element with generalized plastic hinges." J. Engrg. Mech., ASCE, 1986, 112(7): 627-641.
6. ElMandooh Galal, K. and Ghobarah, A. "Flexural and shear hysteretic behaviour of reinforced concrete columns with variable axial load," Eng. Struct., 2003, 25(11): 1353-1367.
7. Wen, Y.-K. "Method for random vibration of hysteretic systems," J. Engrg. Mech. Div., ASCE, 1976, 102(EM2): 249-263.
8. Kunnath, S. K., Reinhorn, A. M. "Model for inelastic biaxial bending interaction of reinforced concrete beam-columns," ACI Structural Journal, 1990, 87(3): 284-291.
9. Casciati, F. "Stochastic dynamics of hysteretic media," Structural Safety, 1989, 6(2-4): 259-269.
10. Wang, C. H. and Y. K. Wen "Evaluation of pre-Northridge low-rise steel buildings. I: Modeling," J. Struct. Engrg., ASCE, 2000, 126(10): 1160-1168.
11. Sfakianakis, M. G. and Fardis, M. N. "Bounding surface model for cyclic biaxial bending of RC sections," J. Engrg. Mech., ASCE, 1991, 117(12): 2748-2769.
12. Sfakianakis, M. G. and Fardis, M. N. "RC Column model for inelastic seismic response analysis in 3D," J. Engrg. Mech., ASCE, 1991, 117(12): 2770-2787.
13. Bousias, S. N., T. B. Panagiotakos, *et al.* "Modelling of RC members under cyclic biaxial flexure and axial force," J. Earthq. Engrg., 2002, 6(2): 213-238.
14. Marante, M. E. and J. Florez-Lopez "Model of damage for RC elements subjected to biaxial bending," Eng. Struct., 2002, 24(9): 1141-1152.
15. Bouc, R. "Modèle mathématique d'hystérésis," Acustica, 1971, 24: 16-25.
16. Park, Y. J., Wen, Y. K., Ang, A. H-S. "Random vibration of hysteretic systems under bi-directional ground motions," Earthq. Engrg. Struct. Dyn., 1986, 14: 543-557.
17. Costa, A. C. and Costa A. G. "Hysteretic model of force-displacement relationships for seismic analysis of structures," National Laboratory for Civil Engineering, Lisbon, 1987.
18. Bousias, S. N., Verzeletti, G., Fardis, M. N. and Gutierrez, E. "Load-path effects in column biaxial bending with axial force," J. Engrg. Mech., ASCE, 1995, 121(5): 596-605.
19. Kawashima Laboratory, Department of Civil Engineering, Tokyo Institute of Technology, <http://seismic.cv.titech.ac.jp/menu.html> (Jan. 15, 2004)